Supplementary Materials for

Establishing a Thermodynamic Landscape for the Active Site of Mo-Dependent Nitrogenase

David P. Hickey[1†], Rong Cai[1†], Zhi-Yong Yang[2], Katharina Grunau[3], Oliver Einsle[3*], Lance C. Seefeldt[2*], Shelley D. Minteer[1*]

Correspondence to: *minteer@chem.utah.edu, lance.seefeldt@usu.edu, einsle@biochemie.uni-freiburg.de

This PDF file includes:

Materials and Methods

Materials

Ethylene glycol diglycidyl ether (EGDGE) was purchased from Polysciences Inc. All other chemicals were purchased from Sigma Aldrich and used as received without further purification. All water used in bioelectrochemical experiments was filtered using an Ultrapure MilliQ system. Ultra-high purity N_2 and Ar were purchased from Airgas company. Acetylene is prepared by the reaction of water on calcium carbide. All experiments were performed under an atmosphere of Ar/H_2 (2.8-3.2%) unless otherwise noted; V-dependent nitrogenase was isolated under an atmosphere of N_2/H_2 (5%).

Growth of *Azotobacter vinelandii* and Purification of Nitrogenase Proteins:

Wild Type Mo-Dependent Nitrogenase, MoFe & FeP

A. vinelandii molybdenum nitrogenase was produced as described previously.[1] Briefly, the cells were grown in 18 L modified Burk medium containing 10 mM NH_4^+. Cells were depressed by centrifugation and resuspension into NH_4^+ free media to enhance nitrogenase expression when the optical density at 600 nm reached 1.5. All of the following steps were carried out under strictly anaerobic condition. Cells were lysed by sonication in the presence of 2 mM sodium dithionite (DT), then the crude extract was separated by anion exchange chromatography (Q-Sepharose, GE Healthcare) over a linear gradient of NaCl (200- 640 mM) to separate MoFe and FeP. His-tagged MoFe was purified over HisTrap HP column (GE Healthcare). The wild-type FeP was further purified by size-exclusion chromatography (Sephacryl S-200, GE Healthcare). All proteins were desalted using a Hitrap desalting column equilibrated with 100 mM MOPS and 2 mM DT, pH = 7.0. Pure protein was concentrated to $\geq$ 20 mg mL^{-1} and shock-frozen in liquid N_2 for future use.

A. vinelandii strains DJ1143 (MoFe protein exressed in a ΔnifB background, resulting in a protein lacking FeMo-cofactor, called apo-MoFe protein), DJ1190 (β-$188^{Ser\rightarrow Cys}$ MoFe protein or S188C MoFe protein), DJ997 (α-$195^{His\rightarrow Gln}$ MoFe protein or H195Q MoFe protein) were grown and nitrogenase MoFe proteins were expressed as reported previously.[2] All MoFe proteins were purified using a previously described metal affinity chromatography protocol. Wild type FeFe protein of Fe-nitrogenase were expressed in *A. vinelandii* strain DJ1255. The details of the construction of *A. vinelandii* strain DJ1255, expression and purification of FeFe protein were done as reported in the literature.[3] The purities of the MoFe proteins isolated were greater than 95% based on the SDS-PAGE analysis using Coomassie blue staining. All MoFe and FeFe proteins except S188C MoFe protein were stored in an 50mM HEPES buffer with ca. 100 mM NaCl and 1 mM dithionite.

Wild Type V-Dependent Nitrogenase, VFe

A. vinelandii VFe protein and its cognate FeP, VnfH, were produced and isolated following established procedures.[4-5] Cells of the *A. vinelandii* type strain (Lipman 1913) were depleted of molybdenum by several generations of growth on Mo-free Burk medium. The culture was then grown with supplementation of sodium vanadate and N_2 gas as the sole nitrogen source, leading to the derepression of the vanadium nitrogenase system. Cells were harvested after approximately 18 h of growth and lysed using an Emulsiflex (Avestin). The lysate was cleared by centrifugation and applied to two consecutive steps of anion exchange chromatography on HiTrap Q (GE Healthcare) and Resource Q (GE Healthcare) under strict exclusion of dioxygen using modified

Schlenk techniques. Both proteins were eluted with NaCl gradients and subsequently concentrated by ultrafiltration. As a final purification step by size exclusion chromatography, VFe protein and VnfH were applied to Superdex 200 and Superdex 75 columns, respectively (GE Healthcare). Pure proteins were concentrated by ultrafiltration and rapidly frozen in liquid N_2 until further use.

Materials Synthesis

High-Molecular Weight Linear Poly(ethylenimine)

High molecular weight linear poly(ethylenimine) (LPEI) was prepared as previously described.[6] Linear poly(2-ethyl-2-oxazoline) (30 g, MW 200,000) was dissolved in an aqueous solution of 3M HCl (1.8 L) and stirred for 5 days at 110 °C. The solution was allowed to cool to room temperature, and the solvent was removed under reduced pressure. The crude polymer was dissolved in H_2O (3 L) at 40 °C and the resulting solution was neutralized using solid NaOH (until pH > 10), causing the polymer to precipitate. The solid polymer was collected by vacuum filtration and recrystallized in H_2O 3 times until the filtrate solution maintains a neutral pH. The purified polymer was dried on a vacuum filter overnight, then dried in a vacuum oven at 50 °C for 24 hours and finally dried at 70 °C for 24 hours. Once cooled to room temperature, the final product was a pale-yellow solid (20 g). Polymer structure and purity were confirmed by ^{1}H-NMR (CD_3OD); δ(ppm) 2.65 (4H, broad *t*).

Pyrene-Modified LPEI

Pyrene-LPEI was synthesized as previously described with minor modification of solvent mixtures used for polymer modification.[1] 1-Pyrenebutyric acid N-hydroxysuccinimide ester (0.27 g, 0.7 mmol) was dissolved in DMSO (5 mL) and added to a stirring solution of MW 80,000 linear poly(ethylenimine) (LPEI, 0.05 g, 1.2 mmol) in MeOH (5 mL) at room temperature. To the stirring reaction mixture was added CH_2Cl_2 (5 mL) to maintain solubility of the modified polymer throughout the duration of the reaction. The reaction solution was stirred for 20 hours at 35 °C in a closed vessel to prevent solvent evaporation. Solvent was removed from the resulting mixture under reduced pressure. The crude product was triturated by first dissolving it in a small amount of DMSO (3-4 mL) and subsequently adding the crude mixture to a rapidly stirring solution of toluene (250 mL), causing the modified polymer to rapidly precipitate. Toluene was decanted and the resulting polymer was washed with THF (30 mL aliquots) to remove unreacted pyrene butyric acid-NHS until the decanted solvent wash was no longer fluorescent under a UV lamp (~10 times). The remaining THF was evaporated under reduced pressure resulting in a flakey yellow-orange solid (0.16 g). Pyrene-LPEI substitution was measured by ^{1}H-NMR ($CDCl_3$) to be 32%.

Bioelectrode Fabrication

Toray Electrode Preparation

Non-wet-proofed Toray paper electrodes were cut into 3 cm x 0.5 cm strips. The strips were then dipped into melted paraffin wax, allowing the wax to cool and solidify so that only a 0.5 cm x 0.5 cm square remained exposed at one end. During electrochemical experiments, the exposed end was coated with pyrene-LPEI/protein films for analysis, while the waxed end was used as an electrochemical connection point for an alligator clip of stainless-steel wire. The purpose of this preparative step is to avoid wicking of the electrolyte solution up the porous

electrode to the electrode-metal led junction, and consequently to prevent corrosion of the metal led.

****It should be noted that, during the preparation of this manuscript, commercial production of non-wet-proofed Toray paper ceased. Similar electrochemical features corresponding to the P-cluster and FeMoco can be observed when pyrene-LPEI/MoFe are coated onto Au and glassy carbon electrodes (albeit with substantially smaller current magnitudes). While we are still exploring alternative carbon paper materials, the most reasonable approximation seems to be AVcarb.*

Pyrene-LPEI/MoFe Film Preparation

Films of pyrene-LPEI/MoFe were prepared as previously described with some modification to solution concentrations.[1] MoFe solution (30 μL, concentration varied slightly 20 – 30 mg mL^{-1} in a 100 mM MOPS buffer, pH 7.0) was added to 70 μL of pyrene-LPEI solution (10 mg mL^{-1} in H_2O), which was subsequently vortexed for 10 s. To the polymer/protein mixture was added a solution of EGDGE (3.75 μL, 8.2% by volume in H_2O), which was again vortexed for 10 s. The pyrene-LPEI/protein/EGDGE mixture (30 μL) was then drop-coated onto a Toray paper electrode (described in SM 3.1) in 10 μL aliquots, which were allowed to cure for 16 h under an atmosphere of Ar/H_2 (3.2%) at room temperature.

Pyrene-LPEI/MoFe/FeP Film Preparation

Films of pyrene-LPEI/MoFe/FeP were prepared in a similar manner to that described in SM Section 3.1. MoFe and FeP mixed solution (30 μL in total, MoFe concentration varied slightly 20 – 30 mg mL^{-1}; FeP concentration varied slightly from 15 – 44 mg mL^{-1} in a 100 mM MOPS buffer, pH 7.0) was added to 70 μL of pyrene-LPEI solution (10 mg mL^{-1} in H_2O), which was subsequently vortexed for 10 s. To the polymer/protein mixture was added a solution of EGDGE (3.75 μL, 8.2% by volume in H_2O), which was again vortexed for 10 s. The pyrene-LPEI/protein/EGDGE mixture (30 μL) was then drop-coated onto a Toray paper electrode (described in SM 3.1) in 10 μL aliquots, which were allowed to cure for 16 h under an atmosphere of Ar/H_2 (3.2%) at room temperature.

Denatured MoFe Control Pyrene-LPEI/MoFe Film Preparation

Films of pyrene-LPEI/denatured MoFe were in a similar manner to that described in SM Section 3.1. MoFe was denatured by exposed to pure O_2 while shaking in a water bath at 30 °C for two hours. Denatured MoFe solution (30 μL, concentration varied slightly 20 – 30 mg mL^{-1} in a 100 mM MOPS buffer, pH 7.0) was added to 70 μL of pyrene-LPEI solution (10 mg mL^{-1} in H_2O), which was subsequently vortexed for 10 s. To the polymer/protein mixture was added a solution of EGDGE (3.75 μL, 8.2% by volume in H_2O), which was again vortexed for 10 s. The pyrene-LPEI/protein/EGDGE mixture (30 μL) was then drop-coated onto a Toray paper electrode (described in SM 3.1) in 10 μL aliquots, which were allowed to cure for 16 h under an atmosphere of Ar/H_2 (3.2%) at room temperature.

Electrochemical Methods

Electrochemical Instrumentation & Data Processing

Electrochemical experiments were performed on a CHI potentiostat using a standard three-electrode cell with a saturated calomel reference electrode (SCE) and a platinum mesh counter electrode and a 0.25 x 0.25 cm Toray paper working electrode. All electrochemical experiments were performed using 100 mM MOPS buffer of pH 7.0 at 25 °C under an atmosphere of Ar/H_2 (3.2%) with less than 3 ppm O_2 unless otherwise noted. Potentials were referenced to a normal hydrogen electrode (NHE) by adding 0.244 V to values measured relative to SCE. All bioelectrode films were electrochemically conditioned prior to use by performing cyclic voltammetry (CV, 5 cycles, 100 mV s^{-1}). All kinetic CVs were performed at 5 mV s^{-1}. Square wave voltammograms (SWVs) were run in a reductive direction with a 20 mV amplitude, 5 mV step potential, and at 30 Hz unless otherwise noted. Step current for SWV data comparing shifts in potential were normalized to 1 as a means of illustrating the shifts in peak potential.

Potentials for P-cluster and FeMoco were determined by SWV, and the average peak potential is reported plus or minus an error compounded from a systematic error of 5 mV (arising from the step potential) plus one standard deviation (where n = 3-6). All SWVs were processed using an open source data analysis program, QSoas, to filter electronic noise and to subtract the baseline value.[7] This was necessary due to the relatively large baseline current corresponding to H^+ reduction by Toray paper at low potentials. Furthermore, an oxidative peak was observed in virtually all SWVs of MoFe/VFe/FeFe-containing films around 0.1 V, which we attribute to the oxidation of either P-cluster of Fe[M]co. Oxidation of this species (i.e. scanning above ~0 V vs NHE) resulted in a complete loss in redox features corresponding to the nitrogenase protein. Consequently, efforts were taken to avoid overoxidation and the onset of this peak was subtracted for clarity. Included below is a representative SWV plot of pyrene-LPEI/MoFe before and after baseline subtraction. Baselines were selected by identifying the tangent of the curve approaching either the oxidizing side of the P-cluster peak or the reducing side of the FeMoco peak. No baseline point was added between peaks. In addition, the precise selection of baseline was found to have very little impact on peak location (only on relative peak height).

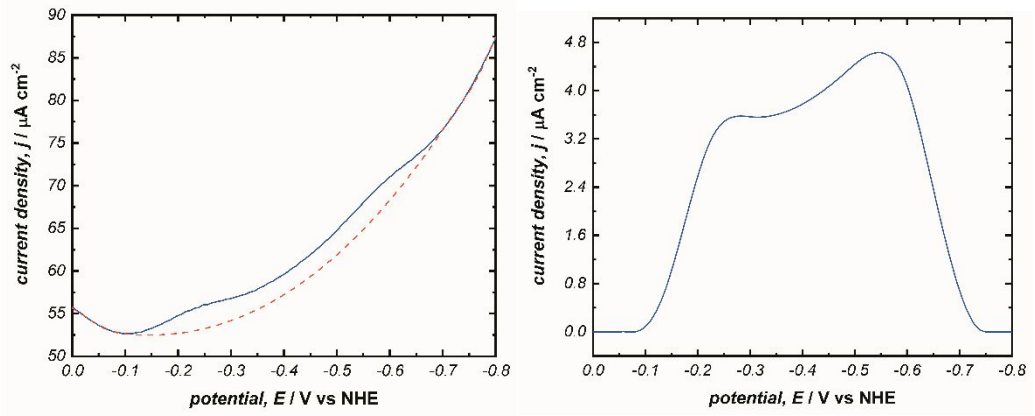

Fig. S1. Representative SWVs of pyrene-LPEI/MoFe films before (left) and after baseline subtraction (right) in QSoas. Experiments were performed using 100 mM MOPS buffer, pH 7.0, 25 °C.

Peak fitting was used to determine the precise value of overlapping peaks observed for FeFe and VFe. Peaks were fit to a gaussian function and the cumulative curve was constructed as the sum of each component curve. Examples of this fitting are demonstrated below for pyrene-LPEI films containing either VFe or FeFe proteins.

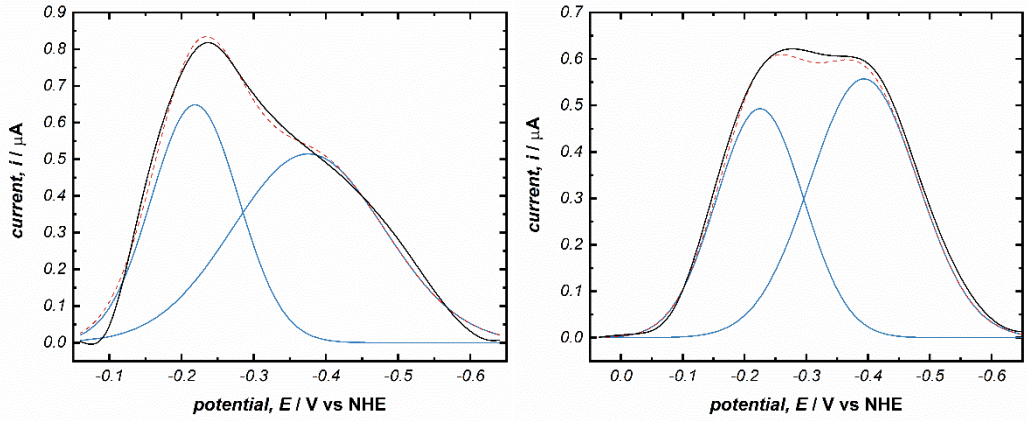

Fig. S2. Representative experimental SWVs (-) of pyrene-LPEI films containing either VFe (left) or FeFe (right), where the fitted component peaks (-) and cumulative fitted peak are overlaid. Peaks were fitted using OriginLab 2018. Experiments were performed using 100 mM MOPS buffer, pH 7.0, 25 °C.

Square Wave Voltammetry Analysis

Unless otherwise noted, all SWVs reported herein were performed at 30 Hz with a step height of 20 mV after extensive optimization of experimental parameters. The step height was found to have minimal impact on the peak current within a range of 10 – 40 mV. Varying frequency was found to impact the peak current linearly for both the peak assigned to P-cluster and FeMoco, which is consistent with an immobilized species on the electrode surface (i.e. immobilized in a thin polymer matrix); however, higher frequencies also resulted in significant peak broadening which eventually leads to overlap between the FeMoco and P-cluster peaks. A frequency of 30 Hz was found to provide an optimal combination of sufficiently high signal and peak resolution.

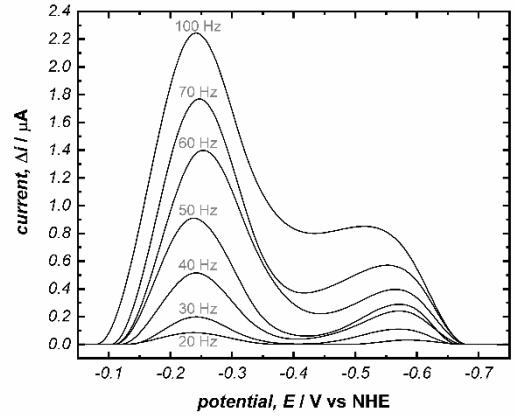

Fig. S3. Representative SWVs of pyrene-LPEI/MoFe films performed at variable frequency with a step height of 20 mV. Experiments were performed using 100 mM MOPS buffer, pH 7.0, 25 °C.

Bulk Electrolysis

Bulk electrolysis cells were assembled under an Ar/H_2 (3.2%) atmosphere. Experiments performed under $^{14}N_2$ were carried out in a sealed three-neck flask to enable precise control of the applied potential. For experiments performed under $^{15}N_2$, an H-cell was used with the working electrode in a sealed compartment and the counter and reference electrodes separated using a Nafion® 212 membrane. The implementation of an H-cell enabled the use of a smaller electrolysis volume (2 mL), which was necessary to reach NH_3 concentrations above the detection limit of ^{1}H-NMR. Due to the added cell resistance associated with the use of an H-cell, a small overpotential was applied (< 100 mV) beyond the desired potential as determined by the measured ohmic drop from uncompensated resistance. This was necessary to ensure that sufficient applied potential was used for activation of the P-cluster.

Electrolysis vessels were degassed after assembly under vacuum at room temperature for 20 min. and filled with either Ar or N_2. This process was repeated three times to ensure all H_2 was removed. The bioelectrodes were conditioned electrochemically prior to electrolysis using CV (5 cycles, 100 mV s^{-1}), and electrolysis was carried out under a constant potential of either -0.25, -0.35, -0.45, -0.55, or -0.65 V vs NHE with rapid stirring using 50 mM MOPS buffer, pH 7.0 at 25 °C. All electrolysis experiments were carried out for 12 hours.

Electrolysis experiments performed under N_2 employed either Ultra High Purity 5.0 Grade $^{14}N_2$ from Airgas Inc. (99.999% purity, ≤ 1 ppm O_2, ≤ 1 ppm H_2O, ≤ 0.5 ppm total hydrocarbon content, ≤ 1 ppm CO, ≤ 1 ppm CO_2) or $^{15}N_2$ from Cambridge Isotope Laboratories Inc. (Lot # I-22779/AR0720534, >99.9% purity; 99.6% isotopic enrichment). Gases were purged through sequential solutions of 0.1 M HCl and 10 mM sodium dithionite to trap any contaminant NH_3 and O_2, respectively (as illustrated below).

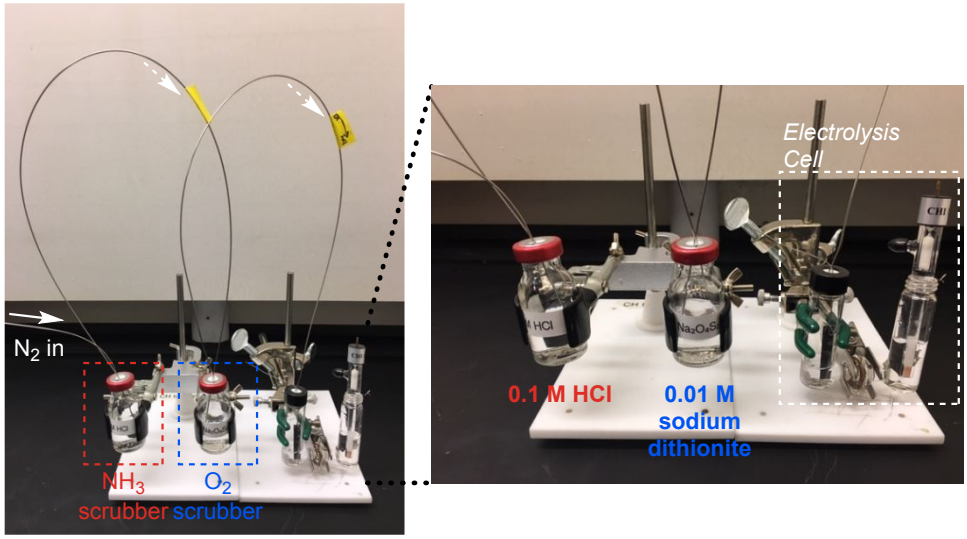

Fig. S4. Schematic diagram of the system used to introduce/purify N_2 gas into bulk electrolysis cells.

It should be noted that the purification system used herein does not contain a method for scrubbing NOx gases that are known to contaminate lecture bottles of $^{15}N_2$. While high temperature copper catalysts commonly employed for Schlenk lines are effective at removing NOx contaminants, such systems often require a substantial amount of source gas to purge the system. Due to the high cost associated with $^{15}N_2$, such a setup was not practical for us; however, previous studies have demonstrated that lecture bottles of $^{15}N2$ from Cambridge Isotope Laboratories Inc.

contain virtually no such contaminants.[8] Furthermore, every effort was made to adhere to the comprehensive workflow recently described by Anderson *et al.* to ensure that the ammonia measured was the result of bioelectrocatalysis.[9] However, some deviations were made due to the additional financial and stability cost associated with the use of an enzymatic electrode. Specifically, quantification of ammonia was done exclusively by a fluorescence assay (described below) due to the small amount of ammonia that could be produced within the enzymatic lifetime under constant potential on the electrode surface (typically ~12 hours before catalytic current decreased to functionally zero). Then confirmation of the ammonia source was accomplished by $^{15}N_2$ labeling experiments.

Bioelectrochemical Production of H_2

MoFe is known to perpetually catalyze H^+ reduction as a critical component of its catalytic cycle; where sequential electron transfer/protonation steps take place from the E_0 to E_4 states of FeMoco followed by relaxation back to E_0, resulting in the production of $2H_2$. To confirm that the observed catalytic current density under pure Ar was in fact the result of H_2 formation, bulk electrolysis was performed under pure Ar and pure N_2 with an applied potential of -0.25 V vs NHE for 20 hours. The head space of the resulting reaction vessels was analyzed by GC-TCD using a Carbonex® 1010 PLOT column (30m x 0.320 mm), at 35 C with an Ar carrier gas at a flow rate of 1 mL min^{-1}. Bulk electrolysis under Ar resulted in 2244 nmol H_2, while bulk electrolysis under N_2 resulted in only 96 nmol H_2. These values are consistent with H^+ reduction being the predominant catalytic reaction under Ar, while being far less significant under N_2.

Experimentally Measured Redox Potentials Compiled

A variety of MoFe mutants were studied as described in the main text. Below is a summary of the redox potentials for the corresponding P-cluster and Fe[M]co clusters as determined herein by SWV as well as their known literature values. There are small discrepancies between the experimentally determined redox potentials reported in this work and literature values determined by EPR spectroscopy (e.g. $E_{P\text{-}cluster}$ for WT MoFe varies by +40 mV from the literature value); however, many of the existing literature values do not report error associated with experimental measurements nor the corresponding Nernstian fitting curves. In some cases error associated with previously reported values may indeed exceed 40 mV (thereby accounting for even the largest discrepancy), it should also be noted that the cationic nature of the LPEI polymer matrix is known to impact the redox potential for small molecules[10] and may slightly alter the redox potential of immobilized proteins. Due to the size of MoFe and the ability of its protein matrix to screen out coulombic effects from the local ionic environment to some extent, we would expect these effects to be minimal and to impact each MoFe isoform uniformly.

Protein, cofactor	*redox potential,*[a] $E_{1/2}$ / V vs NHE	*literature potential,* $E_{1/2}$ / V vs NHE
MoFe (WT)		
P-cluster	-0.23 +/- 0.01	
	-0.26 +/- 0.01 (pH 7.6)	-0.30 (pH 7.5)[b]
FeMoco	-0.59 +/- 0.01	-0.60 (isolated cofactor)[c]
MoFe (βS188C)		
P-cluster	-0.269 +/- 0.009	-0.39 (pH 8.0)[d]
FeMoco	-0.60 +/- 0.01	
MoFe (βH195Q)		
P-cluster	-0.238 +/- 0.006	
FeMoco	-0.56 +/- 0.01	
MoFe (Apo)		
P-cluster	-0.187 +/- 0.007	
FeMoco	*not observed*	*NA*
VFe		
P-cluster	-0.256 +/- 0.008	
FeVco	-0.38 +/- 0.02	
FeFe		
P-cluster	-0.26 +/- 0.02	
FeFeco	-0.40 +/- 0.01	
MoFe (w FeP; active)		
P-cluster	*not observed*	-0.390 (pH 8.0)[e]
FeMoco	-0.43 +/- 0.02	*not reported*
MoFe (intermediate)[g]		
P-cluster	-0.23 +/- 0.01	
FeMoco	-0.43 +/- 0.02	-0.48 (pH 8.0)[f]
MoFe/FeP/MgADPAlF$_4^-$		
P-cluster	*not observed*	
FeMoco	-0.39 +/- 0.03	

[a]*All potentials were determined by SWV at a frequency of 30 Hz using 100 mM MOPS, pH 7.0 at 25 °C under an atmosphere of Ar/H_2 (3.2%)*

[b]Hagen, *Eur. J. Biochem.* **1993**, *212*, 51-61

[c]Schultz, *J. Am. Chem. Soc.* **1985**, *107*, 5364-5368

[d]Seefeldt, Biochemistry, **1999**, *38*, 5779-5785

[e]Seefeldt, *Biochemistry,* **1997**, *36,* 12976-12983

[f]Watt, Biochemistry, **1980**, *19*, 4926-4936

[g]Measured under pure Ar (in the absence of H_2), resulting in an active form of FeMoco, and a resting form of the P-cluster

Table S1. Compiled redox potentials of nitrogenase mutants.

In addition to the table of SWV-derived potentials, we have included a comparison of representative SWVs for the WT, H195Q, and S188C isoforms of MoFe. This data highlights the impact of S188C and H195Q mutations on the redox potential of P-cluster and FeMoco, respectively.

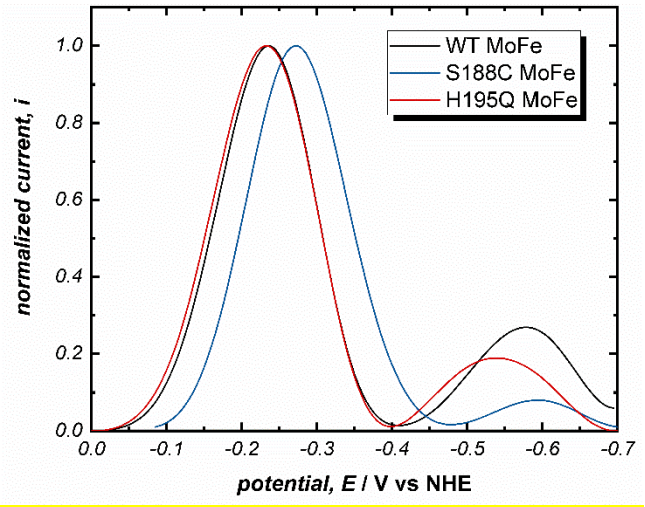

Fig. S5. Representative normalized SWVs of pyrene-LPEI/MoFe films using either WT MoFe (—), βS188C MoFe (—), or βH195Q MoFe (—). Experiments were performed at 30 Hz with an amplitude of 20 mV using 100 mM MOPS buffer, pH 7.0, and 25 °C.

Pyrene-LPEI-Based Electrochemical Interface

Cross-linked films of pyrene-LPEI were examined using confocal fluorescence microscopy (using a Nikon A1R confocal scanning laser fluorescence microscope) to determine the films' thickness in a hydrated form (where films were observed via fluorescence from pyrene moieties). Hydrated film measurements were taken on films coated onto glass microscopes slides where hydration was accomplished by soaking slides in 50 mM MOPS buffer, pH 7.0 at 25 °C for five minutes prior to measurements. By compiling cross-sectional images in the z-plane of 1 μm, we generated a three-dimensional image of pyrene-LPEI films (below). The resulting images suggest a film thickness of 10 – 20 μm.

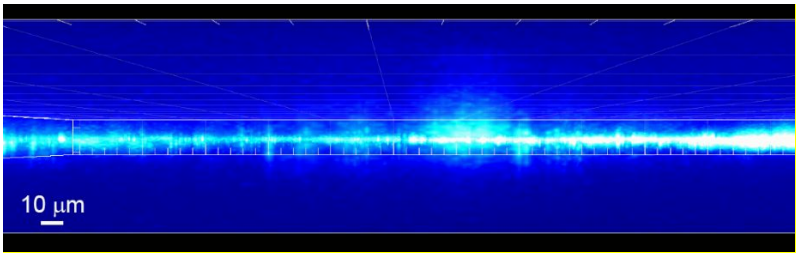

Fig. S6. Representative confocal fluorescence image of hydrated pyrene-LPEI in the z-plane. Fluorescence indicates localized pyrene moieties and serves as an approximation of film thickness.

The precise mechanism by which pyrene-LPEI films enable a coherent electrochemical interface with MoFe (among other metalloenzymes) remains under investigation. Based on our previous work, proteins immobilized in pyrene-LPEI were reported to retain a higher residual activity when compared to other common hydrogels.[1] According to the confocal fluorescence data presented above, the hydrated film thickness of cross-linked pyrene-LPEI is substantially smaller than many other LPEI hydrogels (pyrene-LPEI is 10 - 20 μm thick while naphthoquinone-modified LPEI is reported to be 210 μm thick[11]). Therefore, our working hypothesis is that there is more active protein in a smaller overall volume which increases the probability that a sufficient amount of

randomly oriented protein will be properly aligned to enable direct electrochemical communication with the cofactors of MoFe.

Ammonia Detection & Quantification

Fluorescence Assay for NH_3 Quantification

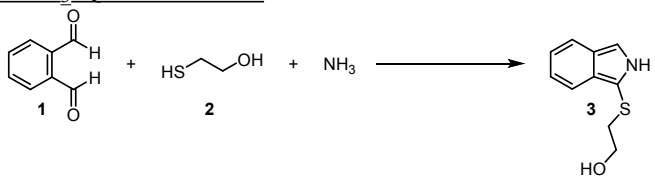

Ammonia production was quantified by fluorescence assay as previously reported.[1, 12] A reagent solution of sodium phosphate buffer (200 mM, pH 7.2, 100 mL), *ortho*-phthalaldehyde (**1**, 270 mg dissolved in 5 mL of ethanol) and 2-mercaptoethanol (**2**, 25 μL) was prepared in the dark prior to each use. Analytical samples (25 μL) were mixed with 1000 μL reagent and incubated for 30 min in dark. Ammonia concentration was correlated to the production of (isoindol-1-yl)thioethanol (**3**) in the above reaction, which was quantified fluorometrically by excitation at 410 nm and recording the emission at 472 nm. All experiments were performed in triplicate and corrected using the results from bulk electrolysis of pyrene-LPEI/denatured MoFe films under N_2 as a baseline.

An additional point should be made that several factors were found to artificially inflate the resulting fluorescence response that were unrelated to the production of NH_3. Two primary contributors were the presence of Tris buffer and the presence of K^+ ions compared to the calibration experiments. The former can be eliminated by adding a buffer exchange step to the end of protein (especially MoFe) isolation to remove Tris buffer that might then leach from the electrode film after coating. The later comes from the use of a saturated KCl solution in the fritted reference electrode. While the second cannot be completely eliminated, thorough cleaning and rinsing of the reference electrodes prior to use in bulk electrolysis aided greatly to mitigating (in fact nearly eliminating) this source of false positive NH_3 detection.

^{1}H-NMR Analysis of $^{14}NH_3$ and $^{15}NH_3$

The NMR spectra were collected at room temperature on a 500 MHz (^{1}H) Varian Inova spectrometer equipped with a cryoprobe. ^{1}H 1-D spectra were collected using a selective excitation pulse for water suppression and a spectral width of 8012.8 Hz (16.0 ppm). Spectra were collected both with and without ^{15}N decoupling during acquisition to demonstrate the absence or presence of ^{15}N-enriched molecules. ^{1}H-NMR signals were averaged over 48 hours in all cases, and baseline subtraction was utilized to account for the overlapping residual peak corresponding to water (after solvent suppression). Due to the proximity of solvent residual peak to that of NH_3, accurate quantification was not possible.

Denatured MoFe Control Experiments for Ammonia Production

Control experiments were performed using pyrene-LPEI films containing denatured MoFe protein (MoFe was denatured as described above). Bulk electrolysis was carried out in a sealed three-neck flask that was assembled under an Ar/H_2 (3.2%) atmosphere. Electrolysis vessels were degassed after assembly under vacuum at room temperature for 20 min. and filled with either $^{14}N_2$ (for fluorescence assays) or $^{15}N_2$ (for ^{1}H-NMR experiments). This process was repeated three times

to ensure all H_2 was removed. The bioelectrodes were conditioned electrochemically prior to electrolysis using CV (5 cycles, 100 mV s^{-1}), and electrolysis was carried out under a constant potential of either -0.25 vs NHE with rapid stirring using 50 mM MOPS buffer, pH 7.0 at 25 °C. All electrolysis experiments were carried out for 12 hours. Fluorescence assays were performed on the $^{14}N_2$ electrolysis solution, which revealed a small background fluorescence signal compared to the electrolysis sample using active MoFe.

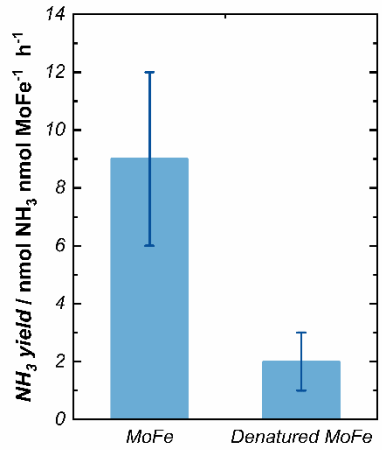

Fig. S7. Ammonia produced from bulk electrolysis using pyrene-LPEI with either active or denatured MoFe protein. Electrolysis was performed at a constant potential of -0.25 V for 12 hours at 25 °C.

Similarly, for control electrolysis experiments performed using denatured MoFe, the $^{15}N_2$ electrolysis solution was acidified and measured by ^{1}H-NMR (as above). While electrolysis using pyrene-LPEI films containing active MoFe resulted in peaks corresponding to $^{15}NH_3$ which were observed by ^{1}H-NMR, no peaks corresponding to $^{15}NH_3$ (nor $^{14}NH_3$) were observed from experiments performed using denatured MoFe after signal averaging of 48 hours. This data is presented in Figure 4B of the primary text.

Investigating Co-Immobilized MoFe/FeP

Controls Using MoFe with Denatured FeP

Control experiments were performed in which, films were prepared using MoFe with two equivalents of denatured FeP. The resulting voltammetry resulted in equal decreases in peak currents for the P-cluster and FeMoco peaks, which is consistent with non-specific binding or the denatured FeP acting as an indiscriminate insulator to both cofactors. Specifically, there is a limited region of the MoFe surface where P-cluster and FeMoco are electrochemically accessible (i.e. within 12 Å of the protein surface). Upon binding of FeP to MoFe, the surface region of MoFe that is electrochemically accessible to the P-cluster is dramatically reduced, while that of FeMoco is relatively unaltered (illustrated below). Based on this observation, we prepared films containing various ratios of MoFe:FeP and studied the resulting films by SWV.

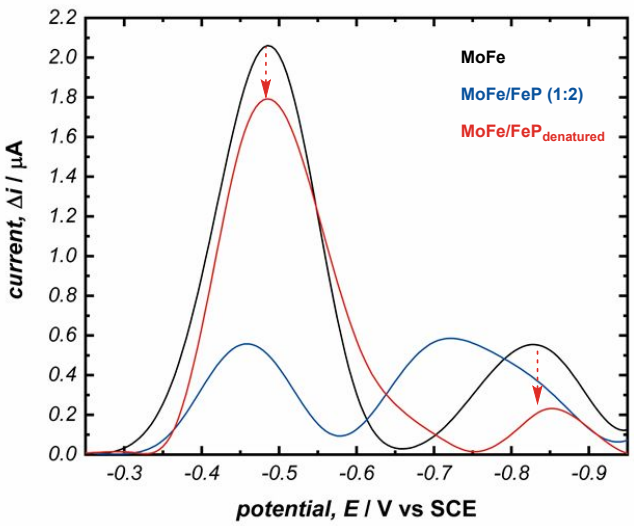

Fig. S8. Representative SWVs of pyrene-LPEI/MoFe films either alone (—), with two equivalents of Fe-protein (—), or containing two equivalents of denatured Fe-protein (—). Experiments were performed using 100 mM MOPS buffer, pH 7.0, with a frequency of 30 Hz at 25 °C.

Similar to CV, the peak current observed in SWV corresponds to the concentration of a redox-active species at the electrode. In the presence of additional equivalents of FeP, a decrease in peak current was observed for both *E1* and *E2*, which is consistent with the excess FeP acting as an electrochemical insulator to the MoFe protein. However, at relatively low concentration of FeP, the decrease in peak current of *E1* (corresponding to the P-cluster) was significantly sharper than that of *E2*. Premixing of the proteins prior to immobilization enables transient association of the nitrogenase complex which enhances the probability of colocalization upon immobilization. Therefore, proximity of FeP to the P-cluster given its native docking site on MoFe would result in preferential blocking of electron transport pathways to an electrode, and consequently a selective loss in current.

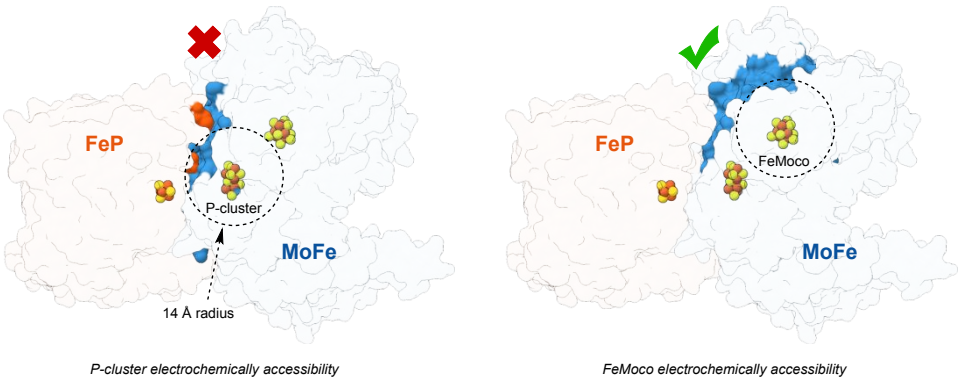

Fig. S9. Scheme highlighting the electrochemically accessible surface to the P-cluster (left) and FeMoco (right) when FeP is bound.

<u>AlF_4 stabilized nucleotide-FeP-MoFe complex</u>

Nucleotide-FeP-MoFe complex was produced as described previously.[13] Briefly, 145 μM $AlCl_3$ and 6 mM NaF were added into 1 mL of an anaerobic ATP-regenerating solution (100 mM MOPS, pH 7.0, 6.7 mM $MgCl_2$, 30 mM creatine phosphate, 5 mM ATP, 0.2 mg mL^{-1} creatine phosphokinase and 1.3 mg mL^{-1} bovine serum albumin) in 9.6 mL vials. Acetylene (C_2H_2)

reduction activity assays with MoFe/FeP (1:16) were performed in an atmosphere of 0.1 atm C_2H_2 and 0.9 atm Ar at 30℃ for 45 min. The reaction mixture was further purified by size-exclusion chromatography (Sephacryl S-200, 1.0 cm × 28 cm, GE Healthcare) equilibrated with 100 mM MOPS, 100 mM NaCl and 2 mM DT, pH = 7.0.

Bioelectrocatalysis of MoFe/FeP

The catalytic cycle for nitrogenase has been extensively studied,[14-17] and the Lowe-Thorneley kinetic model illustrates that the initial stage of catalytic turnover involves a series of alternating one-electron transfer/protonation steps to FeMoco as it is converted from the E_0 to E_4 state prior to binding of N_2.[14-15] In the absence of N_2, FeMoco relaxes from E_4 to E_2 and subsequently the E_0 state while releasing two molecules of H_2; consequently, nitrogenase perpetually generates H_2 under turnover conditions in the absence of an alternative substrate. In order to determine the impact of MgATP on MoFe with FeP during catalytic turnover, we employed slow scan rate cyclic voltammetry on films containing 2:1 FeP-MoFe. Under an atmosphere of Ar with 3% H_2, negligible catalytic current was observed for FeP-MoFe films in the absence of MgATP. However, upon addition of 2.5 mM MgATP, a catalytic current response was observed that is consistent with a persistent background reduction of H^+ described in the Lowe-Thorneley model for the native nitrogenase complex. While this data does not provide implications regarding the structure of native versus immobilized nitrogenase, it does suggest that immobilized FeP-MoFe exhibits similar kinetic and thermodynamic characteristics to the native complex.

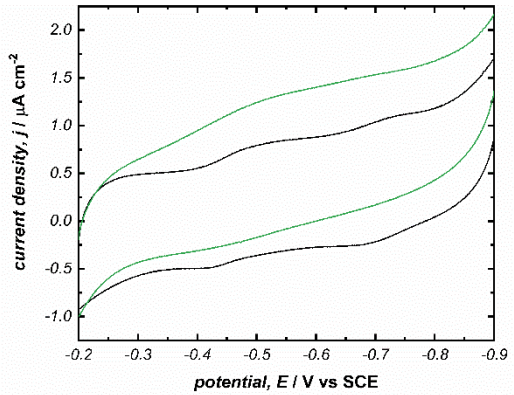

Fig. S10. Representative cyclic voltammogram of pyrene-LPEI films coated with MoFe and FeP (1:2) in the absence (▬) and presence (▬) of 5 mM MgATP. Experiments were performed under a Ar/H_2 (3%) atmosphere, and CVs were performed at 5 mV s^{-1} using 100 mM MOPS buffer, pH 7.0, and 25 °C.

Non-Electrochemical Activity Assay of Immobilized Nitrogenase (MoFe/FeP)

To ensure that immobilized MoFe and FeP proteins maintained their native conformation upon immobilization, non-electrochemical activity assays were performed on immobilized MoFe/FeP (1:16) and compared to the activity of homogeneously dissolved MoFe and FeP. Specific activity was determined using acetylene as a substrate as previously described.[18] Acetylene assays were performed in 9.6 mL vials (septum-sealed) that contained 1 mL of an anaerobic ATP-regenerating solution (100 mM MOPS, pH 7.0, 6.7 mM $MgCl_2$, 30 mM creatine phosphate, 5 mM ATP, 0.2 mg mL^{-1} creatine phosphokinase and 1.3 mg mL^{-1} bovine serum albumin). Acetylene (C_2H_2) reduction activity assays were performed in an atmosphere of 0.1 atm

C_2H_2 and 0.9 atm Ar. The product, ethylene, was quantified by gas chromatography-flame ionization detector (GC-FID) analysis (on a HP PLOT-Q column using He as the carrier gas). All activity assays (chemically and electrochemically driven) were performed in triplicate and the mean values are reported plus/minus one standard deviation.

For the homogeneously dissolved, non-electrochemical nitrogenase activity assay, a MoFe/FeP protein ratio of 1:16 was used (0.1 mg MoFe protein per assay). For the immobilized, non-electrochemical nitrogenase activity assay, pyrene-LPEI/MoFe/FeP films were prepared as described above, using a MoFe/FeP protein ratio of 1:16 (0.19 mg MoFe per assay). Based on the preparation described above, all of the pyrene-LPEI/protein/EGDGE mixture (100 μL) was drop-coated onto the bottom of a septum-sealed vial, which was allowed to dry for 16 h under an atmosphere of Ar/H_2 (3.2%) at room temperature.

	electron donor	*specific activity* / nmol C_2H_4 min^{-1} mg^{-1} MoFe
MoFe/FeP (1:16), dissolved	DT	1410 +/- 90
MoFe/FeP (1:16), immobilized	DT	5.2 +/- 0.6
MoFe(denatured)/FeP (1:16), immobilized	DT	0
MoFe, immobilized	electrode	1.1 +/- 0.2

**proteins immobilized in pyrene-LPEI films*

Table S2. Activity assay (chemically and electrochemically driven) using acetylene as a substrate for nitrogenase (or MoFe).

The resulting assays indicate that 0.3-1.0% of MoFe/FeP maintains activity upon immobilization, which is consistent with previously reported specific activity assays for immobilized versus homogeneously dissolved oxidoreductase enzymes (i.e. laccase).[1] Provided that reversible FeP association to MoFe is necessary for catalytic turnover using a chemical reductant, the observed product formation indicates that a portion of MoFe and FeP must be in their native conformation. In order to correlate the chemically determined specific activity with our electrochemical results, electrolysis was performed using pyrene-LPEI/MoFe films under Ar in the presence of 10% acetylene at -0.6 V and 25 °C for one hour (680 mC of charge passed).

The resulting ethylene was detected as described above, and the corresponding specific activity was significantly lower than that of immobilized nitrogenase (MoFe/FeP) using dithionite as an electron donor. Despite the decrease in specific activity, the ability to convert acetylene to ethylene using a chemical and electrochemical reductant suggests that the observed electrochemical signal is most likely caused by MoFe in its native conformation. Furthermore, the lack of any detectable ethylene formation when denatured MoFe was used (chemical or electrochemical system), demonstrates that dissociated or reconfigured Fe clusters are not likely to cause residual catalytic activity under the conditions described here.

References

1. Hickey, D. P.; Lim, K.; Cai, R.; Patterson, A. R.; Yuan, M.; Sahin, S.; Abdellaoui, S.; Minteer, S. D., Pyrene hydrogel for promoting direct bioelectrochemistry: ATP-independent electroenzymatic reduction of N2. *Chem. Sci.* **2018,** *9* (23), 5172-5177.

2. Christiansen, J.; Goodwin, P. J.; Lanzilotta, W. N.; Seefeldt, L. C.; Dean, D. R., Catalytic and Biophysical Properties of a Nitrogenase Apo-MoFe Protein Produced by a nifB-Deletion Mutant of Azotobacter vinelandii. *Biochemistry* **1998,** *37* (36), 12611-12623.

3. Harris, D. F.; Lukoyanov, D. A.; Shaw, S.; Compton, P.; Tokmina-Lukaszewska, M.; Bothner, B.; Kelleher, N.; Dean, D. R.; Hoffman, B. M.; Seefeldt, L. C., Mechanism of N2 Reduction Catalyzed by Fe-Nitrogenase Involves Reductive Elimination of H2. *Biochemistry* **2018,** *57* (5), 701-710.

4. Sippel, D.; Schlesier, J.; Rohde, M.; Trncik, C.; Decamps, L.; Djurdjevic, I.; Spatzal, T.; Andrade, S. L. A.; Einsle, O., Production and isolation of vanadium nitrogenase from Azotobacter vinelandii by molybdenum depletion. *JBIC Journal of Biological Inorganic Chemistry* **2017,** *22* (1), 161-168.

5. Rohde, M.; Trncik, C.; Sippel, D.; Gerhardt, S.; Einsle, O., Crystal structure of VnfH, the iron protein component of vanadium nitrogenase. *JBIC Journal of Biological Inorganic Chemistry* **2018,** *23* (7), 1049-1056.

6. Hickey, D. P., Ferrocene-Modified Linear Poly(ethylenimine) for Enzymatic Immobilization and Electron Mediation. In *Enzyme Stabilization and Immobilization: Methods and Protocols*, Minteer, S. D., Ed. Springer New York: New York, NY, 2017; pp 181-191.

7. Fourmond, V.; Hoke, K.; Heering, H. A.; Baffert, C.; Leroux, F.; Bertrand, P.; Léger, C., SOAS: A free program to analyze electrochemical data and other one-dimensional signals. *Bioelectrochemistry* **2009,** *76* (1), 141-147.

8. Dabundo, R.; Lehmann, M. F.; Treibergs, L.; Tobias, C. R.; Altabet, M. A.; Moisander, P. H.; Granger, J., The Contamination of Commercial 15N2 Gas Stocks with 15N–Labeled Nitrate and Ammonium and Consequences for Nitrogen Fixation Measurements. *PLoS ONE* **2014,** *9* (10), e110335.

9. Andersen, S. Z.; Čolić, V.; Yang, S.; Schwalbe, J. A.; Nielander, A. C.; McEnaney, J. M.; Enemark-Rasmussen, K.; Baker, J. G.; Singh, A. R.; Rohr, B. A.; Statt, M. J.; Blair, S. J.; Mezzavilla, S.; Kibsgaard, J.; Vesborg, P. C. K.; Cargnello, M.; Bent, S. F.; Jaramillo, T. F.; Stephens, I. E. L.; Nørskov, J. K.; Chorkendorff, I., A rigorous electrochemical ammonia synthesis protocol with quantitative isotope measurements. *Nature* **2019,** *570* (7762), 504-508.

10. Meredith, M. T.; Hickey, D. P.; Redemann, J. P.; Schmidtke, D. W.; Glatzhofer, D. T., Effects of Ferrocene Methylation on Ferrocene-Modified Linear Poly(ethylenimine) Bioanodes. *Electrochim. Acta* **2013,** *92* (0), 226-235.

11. Milton, R. D.; Hickey, D. P.; Abdellaoui, S.; Lim, K.; Wu, F.; Tan, B.; Minteer, S. D., Rational design of quinones for high power density biofuel cells. *Chem. Sci.* **2015,** *6* (8), 4867-4875.

12. Milton, R. D.; Cai, R.; Sahin, S.; Abdellaoui, S.; Alkotaini, B.; Leech, D.; Minteer, S. D., The In Vivo Potential-Regulated Protective Protein of Nitrogenase in Azotobacter vinelandii Supports Aerobic Bioelectrochemical Dinitrogen Reduction In Vitro. *J. Am. Chem. Soc.* **2017,** *139* (26), 9044-9052.

13. Renner, K. A.; Howard, J. B., Aluminum Fluoride Inhibition of Nitrogenase: Stabilization of a Nucleotide Fe-Protein MoFe-Protein Complex. *Biochemistry* **1996,** *35* (17), 5353-5358.

14. L E Mortenson, a.; Thorneley, R. N. F., Structure and Function of Nitrogenase. *Annu. Rev. Biochem* **1979,** *48* (1), 387-418.

15. Burgess, B. K.; Lowe, D. J., Mechanism of Molybdenum Nitrogenase. *Chem. Rev.* **1996,** *96* (7), 2983-3012.

16. Hoffman, B. M.; Lukoyanov, D.; Dean, D. R.; Seefeldt, L. C., Nitrogenase: A Draft Mechanism. *Acc. Chem. Res.* **2013,** *46* (2), 587-595.

17. Hoffman, B. M.; Lukoyanov, D.; Yang, Z.-Y.; Dean, D. R.; Seefeldt, L. C., Mechanism of Nitrogen Fixation by Nitrogenase: The Next Stage. *Chem. Rev.* **2014,** *114* (8), 4041-4062.

18. Milton, R. D.; Cai, R.; Abdellaoui, S.; Leech, D.; De Lacey, A. L.; Pita, M.; Minteer, S. D., Bioelectrochemical Haber–Bosch Process: An Ammonia-Producing H2/N2 Fuel Cell. *Angew. Chem. Int. Ed.* **2017,** *56* (10), 2680-2683.